Journal of Medicinal and Aromatic Plant Sciences 41(1-4), 2019; 39-49

Valorization of processed residue of plant biomass as nanocellulosic material

DISHA MISHRA[1] • RAGHVENDRA PRATAP SINGH • PAORABI DAS • ASHA SINGH[1] • VARSHA PANDEY[1] • PV AJAYA KUMAR[2] • PUJA KHARE[1]*

Article History

Received: November 05th, 2019
Revised: December 2nd, 2019
Accepted: December 2nd, 2019

Key Words

CNF
Cymbopogon winterianus
Musa acuminata
Saccharum officinarum
TEMPO oxidation

ABSTRACT

Residual biomass of Cymbopogon winterianus (Citronella), Saccharum officinarum (Sugarcane bagasse) and Musa acuminata (Banana pseudo stem) were used as raw materials to produce nanofibrillar cellulose. Cellulose was extracted by bleaching treatments and, cellulose nanofibrils (CNFs) were isolated by ultrasonication assisted TEMPO oxidation. Structure, morphology and thermal stability of the isolated CNFs were studied by Fourier transform-infrared (FT-IR) spectroscopy, X-ray diffraction (XRD), Scanning electron microscopy (SEM) and Thermogravimetric analysis (TGA), respectively. Swelling properties of the extracted CNFs were assessed at different pH. The aggregation and sedimentation behaviour of CNFs were evaluated at different salt concentration by measuring transmittance.The CNF isolated from bagasse was found to be more crystalline than those obtained from Citronella and banana stem biomass. Maximum swelling index was observed at neutral pH followed by alkaline pH. Swelling was prominent in Musa acuminate and Saccharum officinarum. Aggregation and sedimentation of CNFs occurred at high salt concentrartion while 10 mM was found to be the critical concentration of NaCl and $CaCl_2$ for a stable dispersion of CNFs in water. This study provides a new approach for the effective utilization of agro-waste as a potential feedstock for the preparation of CNFs and their use in augmentation of advanced structural nanomaterials.

© CSIR-Central Institute of Medicinal and Aromatic Plants, Lucknow-226015

INTRODUCTION

Lignocellullosic residues generated through agriculture is the chief ingredient of organic waste. However, the burning of these waste matter creates severe environmental threats, which ultimately affect human health. Utilization of these residual biomass for the construction of smart renewable resources is one of the solution to overcome this problem, because of their biodegradable, inexhaustible and nontoxic nature. With the increasing attention on sustainable and environment-friendly materials, these agro-wastes could be used for the isolation of natural polymers such as cellulose. Plant-based cellulose

[1]Agronomy and Soil Science Division, CSIR-Central Institute of Medicinal and Aromatic Plants, Lucknow-226015, India.
[2]Analytical Division, CSIR-Central Institute of Medicinal and Aromatic Plants, Lucknow-226015, India.
*Corresponding author, E-mail: kharepuja@rediffmail.com
Doi: https://doi.org/10.62029/jmaps.v41i1.Mishra

nanofibrils(CNFs) have attracted a great deal of interest in the nanocomposite field because of their appealing intrinsic properties such as nanoscale dimensions, high surface area, unique morphology, low density, and high mechanical strength. Cellulose exists in plants in the form of cellulose aggregates, i.e., cellulose nanofibrils, which have a typical diameter of 10–50 nm and are several micrometers in length [18]. Due to their unique super molecular structure, CNFs find application in many fields, such as optoelectronic devices, packaging, and pharmacy [21]. However, the chemical composition of these fibres varies with the source material, age and extraction method.CNFs can be obtained through mechanical treatments such as high pressure homogenization [30], high intensity ultrasonication [5], cryocrushing [1], microfluidization[11], grinding or/and chemical treatments such as typical acid hydrolysis, TEMPO-mediated oxidation, and enzymatic hydrolysis [27]. TEMPO-mediated oxidation is the most used method for the extraction of CNFs[2]. TEMPO catalyzed oxidation of pulp has been found to be an efficient chemical pre-treatment for the production of nanofibrillated cellulose (CNF) [28].The oxidation of the hydroxymethyl groups of cellulose to carboxylates via aldehydes can drastically reduces the energy consumption during the ultrasonic treatment. Oxidation is most effective when there is an abundant availability of non-oxidized surface on fibers. Some fibril surfaces in the cellulose fibers are resistant to TEMPO catalyzed oxidation [31]. Amorphous cellulose is easier to oxidize than crystalline cellulose as the former is accessible to water [17]. The oxidized pulp can be converted to a transparent gel CNF by an ultrasonic treatment [24]. However, the sonication method generates sufficient energy through cavitation, which results in the disintegration of micronsized cellulose fibers into nanofibers. Due to presence of complicated interfibrillar hydrogen bonds in plant cellulose, this method produces aggregated nanofibers with a wide distribution in width. TEMPO oxidized fibers have high surface anionic charge, with good dispersion at very low consistency in an aqueous system. It is expected that the charge properties of CNF surface vary depending on the salt type and salinity, affecting the dispersion or aggregation of the CNF suspension. Hence, it is essential to emphasize the fundamental properties of individual fibrils regarding its colloidal stability without any agglomeration or sedimentation in aqueous systems. Colloidal stability of nanocelluloses in water has been determined based on the Derjaguin–Landau–Verwey–Overbeek (DLVO) theory. This theory explains that chemical factors, such as pH and electrolyte concentration, can decrease the thickness of the electrical double layers of colloids and bring about aggregation of colloids through Brownian motion.

In the Indian aroma industry, *Cymbopogon winterianus* (Citronella) is the most widely cultivated species. *Saccharum officinarum (*Sugarcane bagasse*)* and *Musa acuminata* (banana pseudo stem) are also cultivated all over India. The residue of *Cymbopogon winterianus* is the resultant aerial biomass from which the essential oil has been extracted by hydro-distillation, whereas the residues of *Saccharum officinarum (*Sugarcane bagasse*)* and *Musa acuminata*(banana pseudo stem) are the by-products of sugar and food processing industries, respectively. The residues are mostly treated as waste and returned to either the agricultural fields or burnt. Until now, no study has been published on the isolation of cellulose nanostructures from *Cymbopogon winterianus* and *Musa acuminata* (banana pseudo stem). However isolation of nano cellulose from *Saccharum officinarum (Sugarcane bagasse)* using acid hydrolysis method is reported [19]. The present study aims towards the conversion of the residue of *Cymbopogon winterianus, Musa acuminate* and *Saccharum officinarum* into biodegradable and renewable value-added nano fibrils by ultrasonication-assisted TEMPO oxidation. The morphology, crystalinity, thermal stability, swelling and dispersion properties of the CNFs were investigated to characterize them for future development of reinforced engineered CNF based nanomaterials for wider applications.

MATERIALS AND METHODS

The waste biomass of citronella after oil extraction was taken from oil extraction unit of CSIR-Central Institute of Medicinal and Aromatic Plants, Lucknow. The residual biomasses of sugarcane bagasse (SB) and banana pseudo stem (BS) were obtained from nearby agriculture fields. The chemicals used in the study were of analytical grade (Merck).

Extraction of cellulose from plant fibres

All plants biomass were oven dried at 80°C for 24 hours, followed by grounding and sieving through 60 mesh size. The dewaxing and delignification process of powdered biomasses were done using toluene/ethanol (2:1 v/v) using soxhlet extraction for 24hours. The dewaxed fibres were filtered and washed with ethanol for 30-60 minutes and dried. For extraction of cellulose fibres, the extractive free plant biomass was subjected to alkylation and bleaching according to the methods previously described [32]. Some amount of isolated cellulosic fibres was stored for analysis. The rest of the sample was freeze-dried (Labconco freeze dryer-free zone 2.5 plus-7522800-USA).

TEMPO-mediated oxidation of cellulose fibres

Oxidation of the extracted cellulose fibres was carried out using TEMPO (2,2,6,6-tetramethylpiperidine-1-oxyl radical) coupled with ultra-sonication. First, the fibres (10g) were soaked in water overnight and then homogenized to obtain a uniform suspension of fibre of 1% consistency. TEMPO (0.11mmol/g) and NaBr (0.617/g) were dissolved in 50 ml deionized water. The pH of the fibre slurry was adjusted between 10-12 using 0.5M NaOH/HCl. The oxidation was initiated by adding NaOCl (3.75 mMol) and TEMPO/NaBr solution to the suspension of fibre. The mixture was oxidized in ultasonicator (Helix-JY-92-IIN, frequency = 20-25kHz, RMS power = 150 W) for 90 minutes[9]. The ultra-sonication was initially carried out for 30, 60, 90 and 120 minutes. After analysing the yield, SEM and XRD data (results are not shown here), ultra-sonication time was optimized for 90 minutes. The reaction was stopped by adding ethanol and the pH was adjusted to 7 using 0.5M HCl after 90 minutes. The fibre slurry was washed with distilled water and then filtered and freeze-dried to quantify the yield of oxidized fibre.

Characterization of plant biomass

The extractive free biomass was characterized for cellulose content [34] hemicelluloses content [16] and lignin content [17]. The yield was calculated using the following equation:

$$\text{Yield}(\%) = (W/Wo) \times 100$$

Where W is the weight of fibre obtained and W_0 is the weight of fibre initially taken.

Fourier Transform Infrared Spectroscopy (FT-IR)

FT-IR was performed on Thermo Scientific (NICOLET-380) infrared spectrophotometer using the KBr method. The nanocellulose samples prepared from different methods were mixed with KBr (1:100 w/w) and pellets were used for recording the spectra in the range of 4000 to 650 cm^{-1} with the resolution of $4cm^{-1}$.

The baseline corrected spectra was used to measure the crystalline index (Cir) as the ratio of the absorption band 1430/900 cm^{-1}. The cellulose Iα fraction was calculated using the following equation

$$\int_{\alpha} Cir = \frac{\text{A750}}{A750 + A710}$$

Estimation of carboxyl content in CNFs

The CNFs sample (0.5g) was immersed in 0.01M HCl to convert the cation into hydrogen ion. To the oxidized suspension, 50 mL distilled water and 30 mL of 0.25 M calcium acetate were added. The mixture was kept undisturbed for two hours and then shaken frequently to facilitate the interchange of ions. 30 mL of the mixture was withdrawn and titrated with 0.01M NaOH using phenolphthalein indicator. The carboxyl content was calculated using the following formula [2].

$$COOH\left(\frac{mmol}{g}\right) = \frac{\left(\frac{80}{30}\right) 0.01\text{M}.\,\text{V(NaOH)}}{\text{m}\left(1 - \frac{\text{w}}{100}\right)}$$

Where, 0.01 M is the concentration of NaOH, V is the volume (ml) of NaOH solution used for titration, m is the weight of treated fibres (g), and w is the moisture content.

Morphology, particle size and zeta potential measurement

The morphological features of the suspension of cellulose nanofibers were assessed under SEM (JEOL, JSM-6490-LB-JAPAN). Acceleration voltages of 15KV and 20 KV were used. A fine layer of gold was sprayed on the samples by an ion sputter coater with a low deposition rate before the analysis. Images were obtained at various magnifications. The nanocellulose suspension at 1% (w/v) was diluted with water at the ratio of 1:100 (v/v) and ultrasonicated for 30 min in an ultrasonic bath (Helix Biosciences -40 kHz frequency, 135 RMS power)and analysis were performed using a Malvern Zetasizer NanoZS (Malvern Instruments, UK). This equipment uses dynamic light scattering to measure the diffusion of particles moving under Brownian motion, and converts this to size and size distribution. It also uses laser Doppler micro-electrophoresis to apply an electric field to the dispersion of particles, which then move with a velocity related to their zeta potential.

X- Ray diffraction (XRD) analysis

The structural (physical) properties of the samples were evaluated by X-ray diffraction analysis, at a scanning rate $3^0 min^{-1}$ on a Rigaku X-ray diffractometer (ULTIMA IV, Rigaku, Japan) from 5-100° with a Cu Kα X-ray source (λ = 1.54056 Å) at a generator voltage 40 kV and a generator current 40 mA. The crystalinity indices (CIXRD) were calculated using Segal equation as follows:

$$CIXRD = \frac{I_{200} - I_{am}}{I_{200}} \times 100$$

Where I_{200} is the peak intensity at the (200) (2q =22.5°) plane and I_{am} is the minimum intensity at the valley between (200) and (101) planes (2q = 18°).

The Scherrer equation was used to calculate the crystal size (nm) of cellulose I structure, with respect to the (200) plane.

$$CS = \frac{0.9\lambda}{Hcos\theta}$$

Where, CS is the crystalline size, λ is the X-ray wavelength, H is the full-width at half-maximum (FWHM) and θ is the Bragg angle at the corresponding lattice plane.

Thermal Properties

The thermal behaviour of CNFs samples was investigated using a Leco TGA 701 in aluminium pans. The samples were scanned from 30-800°C at a heating rate of 10°C/min under nitrogen atmosphere.

Swelling index

The swelling index was determined by calculating the volume occupied by the sample before and after swelling. For measurement of swelling ratio, the dried fibers were pre-weighed and then were immersed in different media with pH 2.1, 6.8 and 9.The change in the level of medium was expressed by the swelling index of fiber in ml/g of the dried weight [4].

Salt effect on dispersion ability

The salts of NaCl and $CaCl_2$ were prepared in distilled water of concentration 10, 100, 200 and 400mM, separately. The dispersion of 0.1% CNF was made using appropriate volume of each solution. The transmittance of all the solutions were taken at 546nm using UV-Vis spectrometer (Spectramax Plus 384 with softmax pro. v. 5.3, USA)[12]. Water was used as blank.

RESULTS AND DISCUSSION

Chemical analysis of biomass

The chemical constituents of biomass under study and the yield of cellulose and nanofibrils are reported in the Table 1. The cellulose content of Sugarcane bagasse (SB) (43±2.3 wt%) was higher as compared to Banana stem (BS) (31±1.2 wt%) and Citronella (35±1.4wt%). This cellulose content is much higher compared to that of the spent grains (15–17 wt%) and comparable to other annual plants i.e. Mengkuang leaves[29], Pineapple leaf[8] and

Barley husks[10]. The *A. tequilana* bagasse is composed of a higher amount of cellulose (45.5±0.1 wt%)[3], which is comparable to the cellulose content of SB.

The hemicellulose content of plants used in this study was higher than *Helicteresisora* plant [7], and lotus leaf stock (19.2%) [6]. 25–35% hemicellulose is reported in the waste of sugarcane bagasse [20].The lignin content (10-13 wt%) was found to be within the range (13–22 wt%) reported in literature[7]. The remaining quantity to reach the 100 wt% corresponds to starch, proteins and sugars like xylose, mannose and galactose, which were not quantified in this study.The yields of cellulose extracted from these wastes ranged from 67-91 wt%, showing maximum yield for SB. The yield of nano fibrils prepared by ultra-sonication assisted TEMPO oxidation ranged 70 to 77 wt%, showing minimum yield for citronella. The differences in the composition were found to be depending on the origin of the fibers, particularly in relation to the contents of lignin and cellulose.

Fourier Transform-InfraRed (FT-IR) analysis and surface charge

It is evidenced from the FT-IR spectra that all the nano fibrils possessed characteristic bands of cellulose (Fig.1). The broadbands between 3650cm^{-1} and 3000cm^{-1} are O-H stretching vibrations, peaks at 2900 cm^{-1} correspond to C-H stretching vibrations, and the peaks around 1650

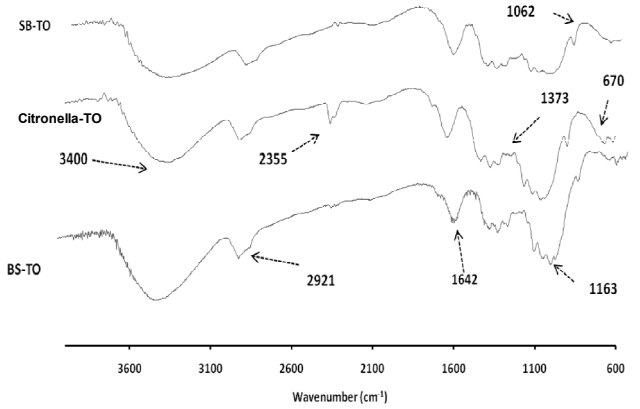

Figure 1: FT-IR of all CNFs.Citronella-TO: TEMPO oxidised nano cellulose extracted from citronella waste material; BS-TO: TEMPO oxidised nano cellulose extracted frombanana stem; SB-TO: TEMPO oxidised nano cellulose extracted fromsugarcane bagasse.

cm^{-1} are due to the deformation vibration of water molecules. Absorption bands in the 1500–800 cm^{-1}spectral region,are attributed to the C-H, O-H,C-O and C =O=C vibrations on the glycosidic ring, representing the fingerprint of cellulose. The increase in intensity of stretching band at 1619 cm^{-1} inCNFs was attributed to the formation of carboxylic group during oxidation. The absorption band, which corresponds to either the acetyl or uronic ester groups of hemicelluloses, appears in the region 1700-1740 cm^{-1}[33]. The crystalline index CI_{ir} (the relative amount of crystalline and amorphous phases), which was estimated from the absorbance ratio of the bands 1427/900 cm^{-1} in the FTIR spectra also confirmed similar crystalline characteristics [36] (Table 2).

Table 1. Chemical constituents of biomass and the yield of cellulose and nanocellulose

	Content (%)			Yield (%)	
	Cellulose	**Hemicellulose**	**Lignin**	**Cellulose**	**TO-CNF**
Citronella	35±1.4	32±1.5	13±1.3	67±1.9	70 ± 1.5
Sugarcane bagasse	43±2.3	36±2.0	13±0.8	91±0.8	77 ± 2.3
Banana pseudo stem	31±1.2	37±2.1	10±0.6	58±1.4	77.5 ± 1.2

Table 2. The properties of nanocellulose obtained in TEMPO oxidation

	Z(mv)	CI_{XRD}	Z value	C_S	COOH (mmol/g)	DS
Citronella	-34.0±2.0	69±2.9	5.22	0.19±.006	0.650±3.1	0.18±0.03
Sugarcane bagasse	-36.1±1.0	65±4.0	3.57	0.24±.004	0.510±4.1	0.52±0.08
Banana pseudo stem	-39.4±2.0	72±1.9	1.62	0.16±.006	0.750±4.9	0.45±0.05

It is known that the ratios of two natural allomorphs i.e., one chain triclinic ($I\alpha$) and two-chain monoclinic ($I\beta$) may influence the crystal pattern of cellulose and also lead to alteration of their other properties significantly. The fractions of $I\alpha$ in CNFs is estimated by FTIR.

Morphology, particle size and zeta potential

Figure 2 shows the comparison of the SEM images of fiber bundles that were separated into individual micro-sized fibers. Upon drying, all the CNFs tend to self-assemble into sub-micron wide and micrometer long fibers. The increase in strong inter-fibrillar attraction via hydrogen bonding among the surface hydroxyl groups of cellulose during the drying process leads to the self-assembly of fibers[15]. Rod shaped structures of fibrils were obtained due to effective oxidation. It is evidenced by the SEM image that the bundle size for SB-TO and BS-TO are almost similar. The constant bundle size might be explained by similarities in the accumulation of charges. Aggregate formation was more pronounced in Citronella-TO, which could be explained by its lower zeta potential. However, the total charge of the bundles was large enough to counteract the short-range attractive van der Waals forces. It could stop the growth of the bundles.

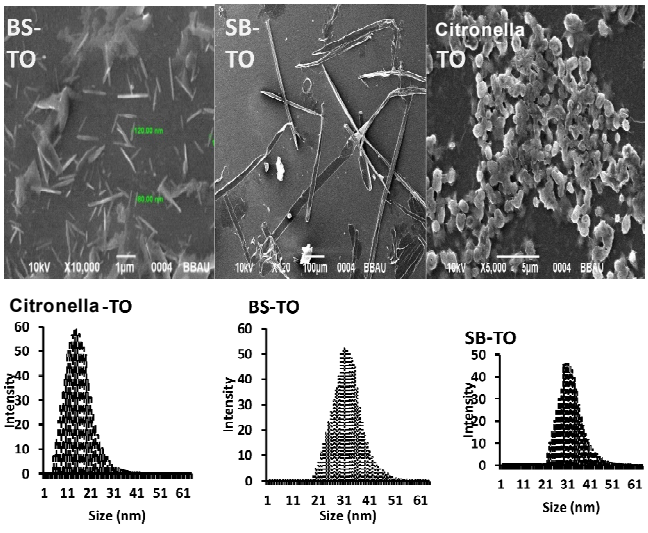

Figure 2: SEM image and particle size analysis of CNFs. Citronella-TO: TEMPO oxidised nano cellulose extracted from Citronella waste material; BS-TO: TEMPO oxidised nano cellulose extracted frombanana stem;SB-TO: TEMPO oxidised nano cellulose extracted fromsugarcane bagasse.

The particle size analyses given in Table 2, revealed that not much variations were observed in the particle size of CNFs. The influence of surface charge on aggregation and size of nano cellulose can be assessed by Zeta potential and functional group analysis of cellulosic fibers. It is observed that Citronella-TO has the lowest values of zeta potential as compared to BS-TO and SB-TO. This is corroborating with the SEM analysis. The degrees of substitution (DS) i.e.the units of carboxylate grafted for each 100 AGU units of cellulose, was the highest for SB-TO.High carboxylic content on the surface may cause more electrostatic repulsion between nanofibrils and help to maintain a homogenous dispersion for a long duration [14].

XRD

Figure 3 shows the comparison of XRD patterns of nanocellulose isolated from the three different sources. All the diffractograms showed two peaks around $2\theta = 16.5^{o}$ and 22.6^{o}, which represent the typical cellulose I structure [23]. The peak at about $2\theta = 16^{o}$ was found to be a combination of two peaks, which indicate the presence of a small amount of cellulose II structure. XRD parameters for crystalinity index (%) and crystal size (nm) of the nanocellulose isolated from various sources are as follows. 82%, 76% and 67% of crystalinity index were obtained in BS-TO, Citronella-TO and SB-TO, respectively. It is comparable to the crystalinity index(75.5 ± 0.7%) of Maize straw [26]. However, The crystalinity of these CNFs were higher than that of other agro-industrial waste such as rice husk [16] and cassava bagasse [25]. The higher crystalline nature of nanocellulose is undoubtedly due to a more efficient removal of non-cellulosic components from the fibers, i.e. the dissolution of amorphous regions, by controlled acid hydrolysis process. Crystal sizes of CNFs from all the three sources were found to be around 5.0 nm. This value of crystal size was in the same range as reported for nanocellulose isolated from maize straw (4.3±0.2 nm)[33]and *Opuntia ficus indica*(5nm) [13]. The results of XRD analysis confirmed that the degree of crystallinity of the nanocellulose depend

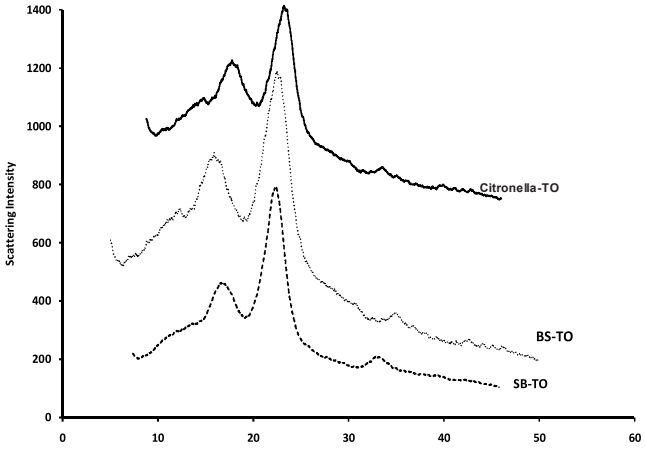

Figure 3: XRD spectra of CNFs. Citronella-TO: TEMPO oxidised nano cellulose extracted from Citronella waste material; BS-TO:TEMPO oxidised nano cellulose extracted from banana stem; SB-TO: TEMPO oxidised nano cellulose extracted fromsugarcane bagasse

on the cellulosic raw material.These results indicate that the ultrasonication assisted TEMPO oxidation employed is adequate to obtain highly crystalline cellulose from these agro-waste materials.

Thermal properties

The thermal behavior of CNFs was investigated using TGA in an inert environment in identical conditions (Fig. 4). Hence, the devolatilization pattern of nanocellulose reflects the variations in its physico-chemical properties (size and texture of the cellulose sample and crystallinity). According to devolatilization pattern, the thermogram of nanocellulose showed three regions. The region I (from 30°C to 180°C) corresponds to dehydration of nanocellulose. The mass loss in this region varied from 9 to 12%. The temperature, where the mass loss deviated from the plateau region (about 200 °C and 250°C) was considered as the onset of region II. Here, the dehydration and depolymerisation of cellulose occurs with the release of volatiles. The mass loss at the end of region II (200/250°C to 404/450°C) varied from 41 to 65%. After region II, the mass loss rate of the cellulosic samples decreased. In region III, the mass loss varied from 10 to 13%. The SB-TO had a lower rate of degradation and maximum char residue. It also had slightly higher degradation temperature as compared to the other

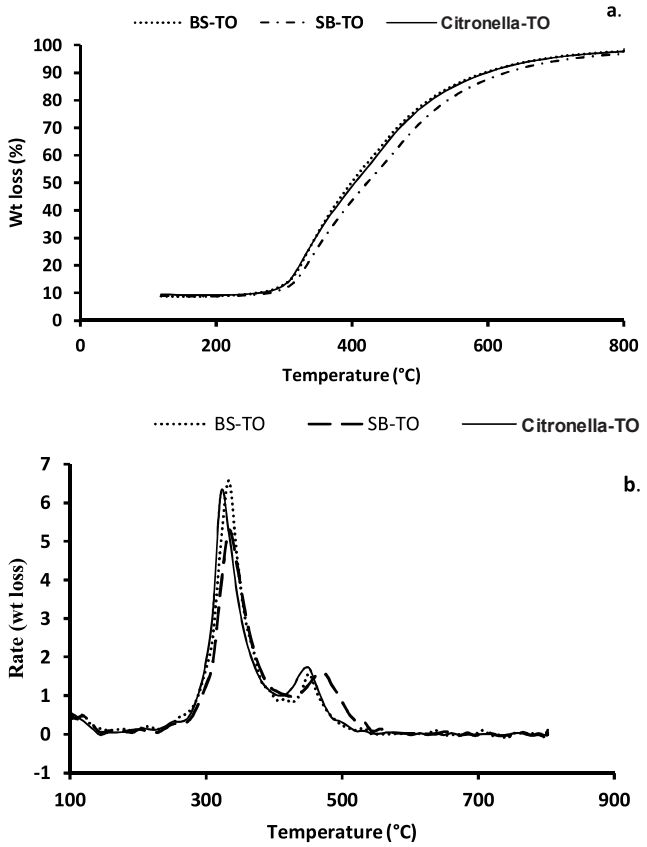

Figure 4: Thermogravinetric analysis of CNFs a. TGA graph b. DTA graph. Citronella-TO: TEMPO oxidised nano cellulose extracted from Citronella waste material; BS-TO: TEMPO oxidised nano cellulose extracted frombanana stem;SB-TO: TEMPO oxidised nano cellulose extracted fromsugarcane bagasse.

two materials. Low degradation temperatures of Citronella-TO and BS-TO an due to the presence of lignin, hemicelluloses and other non-cellulosic segment which decompose at low temperature [19].

Swelling properties

The swelling of cellulose and nano cellulose fibrils at different pH were assessed. As all the cellulose extracted from different biomass possessed more or less similar behaviours, only swelling index of LG-cellulose was showed for comparison. It is evidenced from Figure 5 that the nanocellulose fibrils have great capacity to absorb water, which occurs rapidly and continuously during the first 60 min. The swelling capacity of oxidized CNF was quite high as compared to cellulosic material.This is due to the surface modification on cellulose during oxidation which reduces the

amount of OH groups necessary for forming hydrogen bonds between adjacent nanofibrils during drying. The swelling properties of CNFwere lower in acidic pH. The swelling properties of each CNF exhibited different trends in different pH. At acidic pH, SB-TO displayed highest swelling among all, while in neutral and basic pHs, BS-TO and Citronella-TO demonstrated higher swelling index, respectively. The liquid absorption depends on the pH of the liquid. This capability is due to the swelling property of oxidized nanocellulose, which have ionisable functional groups. The swelling is lower at pH 9 compared to pH 6.8 due to larger concentrations of salt, which leads to charge shielding of the carboxylate ions. The ionic strength is thus lower in the neutral swelling medium, compared to the alkaline and acidic media. Since the pK of the weak poly acid is about ~4.7 and ionization occurs above this pH, a low swelling was observed.Swelling index indicates that these materials can act as drug delivery agents, in which the drug is not released at low pH values in the stomach but rather at high pH values in the upper small intestine. They may act as good pH responsive materials.

Salt effect on the dispersion stability

Dispersion stability of CNFs in water was also investigated to elucidate critical salt concentration for aggregation. The obtained light transmittances showed that the stability of the 0.1 % CNF/water dispersion was affected by NaCl and $CaCl_2$ concentrations. Figure 6 shows the light transmittance spectra of 0.1 % w/v dispersions of CNFs prepared under the same disintegration conditions under different salt concentrations. Low light transmittances are caused by the presence of aggregation with sizes greater than the light wavelengths. The CNF with salt solution >100mM had < 90% light transmittance at 650 nm, whereas with salt solution <100mM had high values of 89% and 95 %, respectively. All CNF elements were stably dispersed in water at NaCl and $CaCl_2$ concentrations of 10mM. However, the CNF dispersion gradually lost transmittance and aggregation became remarkable with the increased salt concentration. The CNF elements partially aggregated in the dispersion at 100 mM NaCl and 100mM $CaCl_2$. Almost all CNFs in the dispersions formed aggregated gel particles at salt concentration > 100mM (Fig. 6). However, the critical aggregation point for monovalent cation is 10mM; BS-TO and SB-TO showed some colloidal stability at 100mM as well. But Citronella-TO started aggregation immediately after the concentrartion exceeded 10mM. This might be due to the development of large number of counter ions on the surface of fibrils by addition of salts which could result in a decrease in the surface charge due to interaction between counter ion and carboxyl

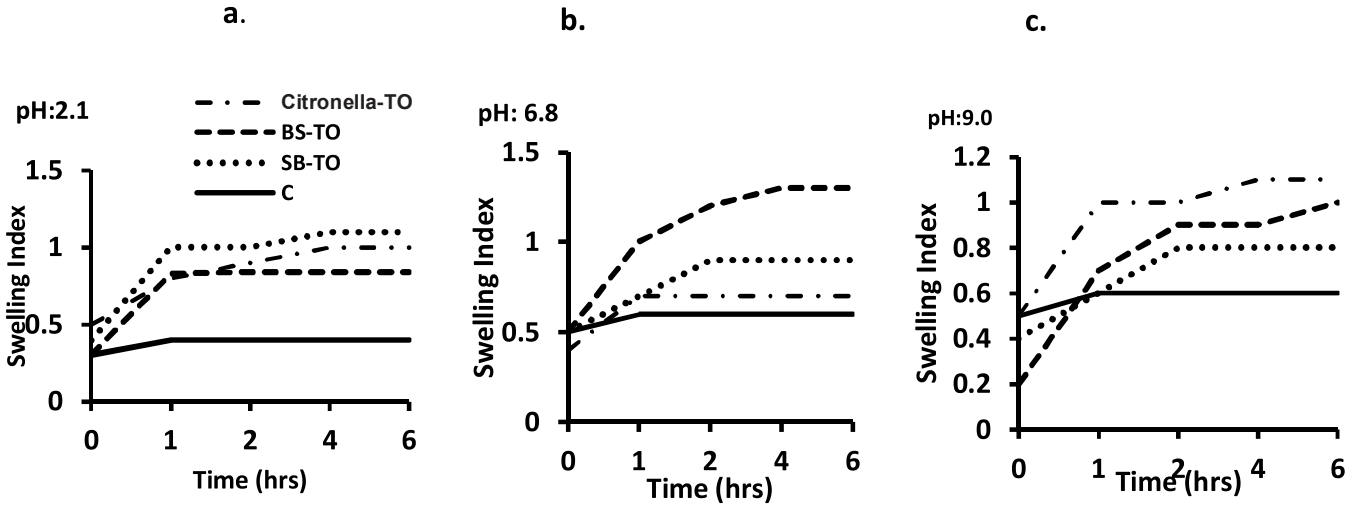

Figure 5: Swelling of nano fibres at different physiological pH i.e. a. at pH 2.1; b. at pH 6.8 and c. at pH 9.0. Citronella-TO: TEMPO oxidised nano cellulose extracted from Citronella waste material; BS-TO: TEMPO oxidised nano cellulose extracted frombanana stem;SB-TO: TEMPO oxidised nano cellulose extracted from sugarcane bagasse, C: cellulose

groups. At higher concentrations of salt or divalent cations, a greater compression of electric double layer occurs, promoting the electrostatic repulsion which leads to aggregation and sedimentation of fibrils. Therefore, due to low surface anionic charge on Citronella-TO, in the case of monovalent cation at low concentration, it is stable while at high salts concentration aggregates are formed due to the compression of electric double layer. However, in case of divalent cation at a low concentration of 10mM, the stability losses due to an immediate decrease in the electrostatic repulsion, leading to sedimentation.

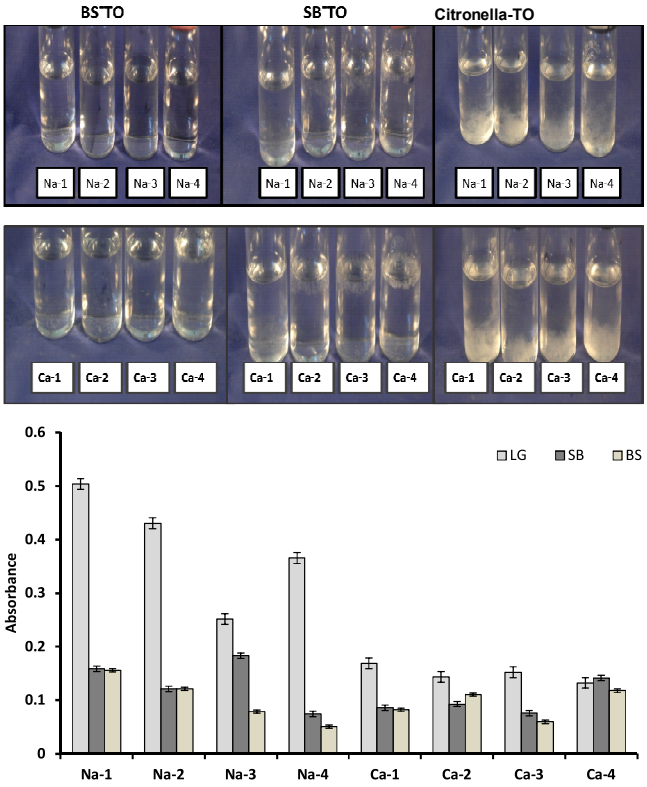

Figure 6: Effect of salt on CNF dispersion. (Na-1,Na-2, Na-3 and Na-4 and Ca-1,Ca-2, Ca-3 and Ca-4 are 10mM, 100mM, 200mM and 400mM concentration of NaCl and $CaCl_2$, respectively.)

CONCLUSION

In this study, we demonstrated the production of cellulose fibres of three different plant residues by ultrasonicated TEMPO oxidation. This process resulted in individualization of plant fibers ranging from 10-15 nm in width and several micrometres in length, with significant amounts of carboxyl groups. The pH-responsive characteristics of these fibres were assessed using swelling index. It is suggested that the poly-anionic characteristics of oxidized cellulosic nanofibers enhanced the swelling property of the nanocellulose structures, which have ionisable functional groups. The nanocellulose gels exhibited a significantly higher swelling degree in neutral and alkaline conditions, compared to an acid environment (pH 4). The pH and salts responsive characteristics of the CNFs could be potentially exploited for the development of new reinforced nanocomposites.

ACKNOWLEDGEMENT

The work was supported by the Council of Scientific &Industrial Research, New Delhi.

REFERENCES

1. Abraham E, Deepa B, Pothan L, Jacob M, Thomas S, Cvelbar U, Anandjiwala R. 2011. Extraction of nanocellulose fibrils from lignocellulosic fibres: a novel approach. *Carbohydrate Polymers* **86** : 1468-1475.

2. Abraham E, Deepa B, Pothen L, Cintil J, Thomas S, John M, Anandjiwala R, Narine S. 2013. Environmental friendly method for the extraction of coir fibre and isolation of nanofibre. *Carbohydrate Polymers*. **92**: 1477-1483.

3. Alonso Gutierrez MDLS. 2005. Valorisation of the bagasse of the tequilana agavae W. cv azul: caractérisation, study of the digestibility and fermentation of sugars. Ph.D Thesis, Agro-Industrial Chemistry Department, Toulouse, France.

4. Amin MCIM, Ahmad N, Halib N, Ahmad I. 2012. Synthesis and characterization of thermo-and pH-responsive bacterial cellulose/acrylic acid hydrogels for drug delivery. *Carbohydrate Polymers*. **88:** 465-473.

5. Chen P, Yu H, Liu Y, Chen W, Wang X, Ouyang M. 2013. Concentration effects on the isolation and dynamic rheological behavior of cellulose nanofibers via ultrasonic processing. *Cellulose* **20** 149-157.

6. Chen Y, Wu Q, Huang B, Huang M, Ai X. 2014. Isolation and Characteristics of Cellulose and Nanocellulose from Lotus Leaf Stalk Agro-wastes. *Bioresources*. **10** : 684-696.

7. Chirayil CJ, Joy J, Mathew L, Mozetic M, Koetz J, Thomas S. 2014. Isolation and characterization of cellulose nanofibrils from Helicteres isora plant. *Industrial Crops and Products*. **59**: 27-34.

8. Dos Santos RM, Neto WPF, Silvério HA, Martins DF, Dantas NO, Pasquini D. 2013. Cellulose nanocrystals from pineapple leaf. A new approach for the reuse of this agro-waste. *Indus Crops Prod* **50**: 707-714.

9. Dufresne A. 2013. Nanocellulose: a new ageless bionanomaterial. *Materials Today*. **16:** 220-227.

10. Espino E, Cakir M, Domenek S, Román-Gutiérrez AD, Belgacem N, Bras J. 2014. Isolation and characterization of cellulose nanocrystals from industrial by-products of Agave tequilana and barley. *Indus Crops Prod* **62**: 552-559.

11. Ferrer A, Quintana E, Filpponen I, Solala I, Vidal T, Rodríguez A, Laine J, Rojas OJ. 2012. Effect of residual lignin and heteropolysaccharides in nanofibrillar cellulose and nanopaper from wood fibers. *Cellulose* **19 :** 2179-2193.

12. Fukuzumi H, Tanaka R, Saito T, Isogai A. 2014. Dispersion stability and aggregation behavior of TEMPO-oxidized cellulose nanofibrils in water as a function of salt addition. *Cellulose*. **21**: 1553-1559.

13. Habibi Y, Mahrouz M, Vignon MR. 2009. Microfibrillated cellulose from the peel of prickly pear fruits. *Food Chem* **115**: 423-429.

14. Iwamoto S., Lee S-H, Endo T. 2013. Relationship between aspect ratio and suspension viscosity of wood cellulose nanofibers. *Polymer J* **46**: 73-76.

15. Jiang F, Hsieh Y-L. 2013. Chemically and mechanically isolated nanocellulose and their self-assembled structures. *Carbohydrate polymers*. **95**: 32-40.

16. Johar N, Ahmad I, Dufresne A. 2012. Extraction, preparation and characterization of cellulose fibres and nanocrystals from rice husk. *Indus Crops Prod* **37**: 93-99.

17. Johnson RK. 2010. TEMPO-oxidized nanocelluloses: Surface modification and use as additives in cellulosic nanocomposites in. *Virginia Polytechnic Institute & State University*.

18. Jonoobi M, Harun J, Tahir PM, Shakeri A, SaifulAzry S, Makinejad MD. 2011. Physicochemical characterization of pulp and nanofibers from kenaf stem. *Materials Lett* **65:** 1098-1100.

19. Kumar A, Negi YS, Choudhary V, Bhardwaj NK. 2014. Characterization of cellulose nanocrystals produced by acid-hydrolysis from sugarcane bagasse as agro-waste. *J Materials Phy Chem* **2:** 1-8.

20. Mandal A, Chakrabarty D. 2011. Isolation of nanocellulose from waste sugarcane bagasse (SCB) and its characterization. *Carbohydrate Polymers*. **86** : 1291-1299.

21. Missoum K, Belgacem MN, Bras J. 2013. Nanofibrillated cellulose surface modification: a review. *Materials* **6:** 1745-1766.

22. Musha Y, Goring D. 1974. Klason and acid-soluble lignin content of hardwoods. *Wood Sci For Prod Res Soc Madison*.

23. Nishiyama Y, Langan P, Chanzy H. 2002. Crystal structure and hydrogen-bonding system in cellulose lâ from synchrotron X-ray and neutron fiber diffraction. *Journal of the American Chemical Society*. **124**: 9074-9082.

24. Okita Y, Saito T, Isogai A. 2009. TEMPO-mediated oxidation of softwood thermomechanical pulp. *Holzforschung* **63**: 529-535.

25. Pasquini D, de Morais Teixeira E, da Silva Curvelo AA, Belgacem MN, Dufresne A. 2010.

Extraction of cellulose whiskers from cassava bagasse and their applications as reinforcing agent in natural rubber. *Indus Crops Prod* **32 :** 486-490.

26. Rehman N, de Miranda MIG, Rosa SM, Pimentel DM, Nachtigall SM, Bica CI. 2014. Cellulose and nanocellulose from maize straw: an insight on the crystal properties. *J Polymers Environ* **22:** 252-259.

27. Sacui IA, Nieuwendaal RC, Burnett DJ, Stranick SJ, Jorfi M, Weder C, Foster EJ, Olsson RT, Gilman JW. 2014. Comparison of the properties of cellulose nanocrystals and cellulose nanofibrils isolated from bacteria, tunicate, and wood processed using acid, enzymatic, mechanical, and oxidative methods. *ACS Appl Mat Interfaces* **6** : 6127-6138.

28. Saito T, Isogai A. 2004. TEMPO-mediated oxidation of native cellulose. The effect of oxidation conditions on chemical and crystal structures of the water-insoluble fractions. *Biomacromol* **5** 1983-1989.

29. Sheltami RM, Abdullah I, Ahmad I, Dufresne A, Kargarzadeh H. 2012. Extraction of cellulose nanocrystals from mengkuang leaves (Pandanus tectorius). *Carbohydrate Polymers*. **88**: 772-779.

30. Stenstad P, Andresen M, Tanem BS, Stenius P. 2008. Chemical surface modifications of microfibrillated cellulose. *Cellulose* **15**: 35-45.

31. Su Y, Burger C, Ma H, Chu B, Hsiao BS. 2015. Exploring the Nature of Cellulose Microfibrils. *Biomacromol* **16** : 1201-1209.

32. Sun R, Sun, 2002. Fractional and structural characterization of hemicelluloses isolated by alkali and alkaline peroxide from barley straw. *Carbohydrate polymers*. **49**: 415-423.

33. Tang Y, Yang S, Zhang N, Zhang J. 2014. Preparation and characterization of nanocrystalline cellulose via low-intensity ultrasonic-assisted sulfuric acid hydrolysis. *Cellulose*. **21**: 335-346.

34. Updegraff DM. 1969. Semimicro determination of cellulose inbiological materials. *Analy Biochem* **32:** 420-424.

35. Van Soest PV, Robertson J, Lewis V. 1991. Methods for dietary fiber neutral detergent fiber and nonstarch polysaccharides in relation to animal nutrition. *J Dairy Sci* **74:** 3583-3597.

36. Wang H, Li D, Zhang R. 2013. Preparation of ultralong cellulose nanofibers and optically transparent nanopapers derived from waste corrugated paper pulp. *Bioresources*. **8:** 1374-1384.